Self-Assembly of Poly(caprolactone-*b*-ethylene oxide-*b*-caprolactone) via a Microphase Inversion in Water

Yue Zhao

The Opening Laboratory for Band-Selective Chemistry, Department of Chemical Physics, University of Science and Technology of China, Hefei, Anhui 230026, China

Haojun Liang

Department of Polymer Science and Engineering, University of Science and Technology of China, Hefei, Anhui, 230026, China

Shenguo Wang

Laboratory of Membranes and Medical Polymers, The Institute of Chemistry, Chinese Academy of Sciences, Beijing, 100080, China

Chi Wu*

Department of Chemistry, The Chinese University of Hong Kong, Shatin, N.T.; Hong Kong

Received: August 22, 2000

Triblock copolymer poly(caprolactone-*b*-ethylene oxide-*b*-caprolactone) (PCL−PEO−PCL) could self-assemble into narrowly distributed flowerlike "core−shell" micelles when its tetrahydrofuran solution was added dropwise into an excess of water. The core was formed via the aggregation of insoluble hydrophobic PCL blocks, while the shell was made of many hydrophilic PEO loops. The formation and stabilization of such micelles were examined by a combination of static and dynamic laser light scattering. The average hydrodynamic size decreased as the dispersion temperature increased, but there was no change in the average radius of gyration, indicating that the temperature dependence of $\langle R_h \rangle$ during heating or cooling was attributed to the conformation change of the PEO block. The composition dependent study revealed that using two short PCL blocks and a long PEO block unexpectedly lead to smaller micelles. The study of their biodegradation in the presence of enzyme Lipase PS shows possible biomedical applications of such formed polymeric micelles.

Introduction

Block copolymers have attracted much attention because of their unique phase behavior in blends and their ability to form polymeric micelle-like "core−shell" nanostructure in a selective solvent, in which only one block is soluble. For example, poly-(ethylene oxide-*b*-propylene oxide) (PEO-*b*-PPO) was one of the most studied diblock copolymers, because at temperatures higher than ∼20 °C, the PPO block is insoluble in water.[1−3] The aggregation of insoluble blocks results in a relatively compact core, while soluble blocks form a swollen protective corona. If the soluble block is much longer than the insoluble block, the aggregates are spherical and are "starlike". On the other hand, if the soluble block is much shorter than the insoluble block, the aggregates are called "crew-cut".[4,5]

For an A−B−A type triblock copolymer, in a solvent selective for the A block, the association of the B blocks yields the brushlike core−shell micelles.[6−8] Recently, we have proposed a simple scaling for such formed nanostructures.[9] On the other hand, if the A block is insoluble, the association of the A blocks could be either an interchain or intrachain one, which makes the problem more complicated. Most of the past studies were concentrated on commercially available triblock copolymer

PPO−PEO−PPO[10] and poly(oxybutylene-*b*-oxyethylene-*b*-oxybutylene).[11−13]

Cosmetic and biomedical applications of these block copolymers, such as in drug delivery and image enhancement, have been proposed.[14−16] However, for fundamental studies, the impurity inside these commercial samples often tarnished the experimental results and their conclusions. To overcome this problem, we prepared a series of poly(ethylene oxide) and poly-(caprolactone) (PCL) block copolymers. Previously, we studied the micelles made of diblock PCL−PEO copolymer and their enzymatic biodegradation.[17,18] In this study, we extended our investigation to a more complicated triblock copolymer PCL−PEO−PCL system. We studied the block length and temperature dependence of the formation and stabilization of these novel polymeric micelles in water. Their enzymatic biodegradation is also evaluated.

Materials and Methods

Materials. Three triblock poly(caprolactone-*b*-ethylene-*b*-caprolactone) (PCL−PEO−PCL) copolymers with different block lengths were synthesized by polycondensation of a prescribed amount of ε-caprolactone (CL) (Janssen Chimica) and poly(ethylene oxide) (Tianjin Eastern Health Materials Factory) at 160 °C for ∼7 h in the presence of stannous octoate

* Corresponding author. Tel: +852 2609 6106. Fax: +852 2603 5057. E-mail: chiwu@cuhk.edu.hk.

Self-Assembly of PCL−PEO−PCL

J. Phys. Chem. B, Vol. 105, No. 4, 2001 **849**

TABLE 1: Characterization of Poly(caprolactone-*b*-ethylene oxide-*b*-caprolactone) (PCL−PEO−PCL) Triblock Copolymers

sample	PCL80	PCL60	PCL40
W_{PEO}/W_{PCL}	20/80	40/60	60/40
$M_{w,chain}$	7.30×10^4	7.50×10^4	4.75×10^4
$M_{w,PCL}$	6.58×10^4	5.80×10^4	2.86×10^4
$M_{w,PEO}$	7.20×10^3	1.70×10^4	1.89×10^4

(Aldrich) as a catalyst. The synthesis details can be found elsewhere.[19] The weight ratio of PCL to PEO (W_{PCL}/W_{PEO}) and the weight-average molar mass (M_w) of these copolymers are listed in Table 1. The samples are narrowly distributed with M_w/M_n < 1.2.
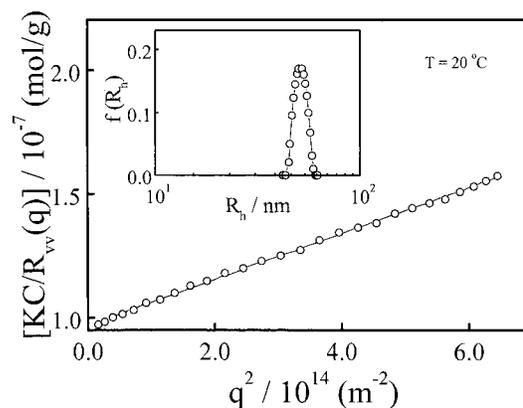
Sample Preparation. The self-assembly of PCL−PEO−PCL was achieved by adding 0.1 mL of copolymer tetrahydrofuran (THF) solution (1.37×10^{-3} g/mL) dropwise into 50 mL of deionized water *without stirring* at 20 °C. Since THF is miscible with water, the diffusion of THF into water resulted in the intrachain contraction and association of the PCL blocks. The soluble PEO blocks tended to stay on the periphery and acted as a protective layer. The trick of *no-stirring* was adopted to reduce the interchain association of the PCL blocks, so that narrowly distributed small micelles could be formed. The trace amount of THF was removed by a low-pressure distillation. The resultant nanoparticle dispersions were clarified by a 0.5 μm Millipore filter to remove dust. The final copolymer concentration was $C = 2.74 \times 10^{-6}$ g/mL.

Laser Light-Scattering. A commercial LLS spectrometer (ALV/SP-125) equipped with an ALV-5000 multi-τ digital time correlator and a He−Ne laser (Uniphase, output power $\cong$ 20 mw at $\lambda = 632.8$ nm) was used. In static LLS, the angular dependence of the excess absolute time-averaged scattered intensity of a dilute dispersion, i.e., the Rayleigh ratio $R_{vv}(q)$, can lead to the weight-averaged molar mass M_w, the second virial coefficient A_2, and the z-averaged root-mean square radius of gyration $\langle R_g^2 \rangle_z^{1/2}$ (or written as $\langle R_g \rangle$),[20] where q is the scattering vector. In this study, the concentration is so low that the extrapolation to infinite dilution was not necessary.

In dynamic LLS, the Laplace inversion of a measured intensity−intensity−time correlation function $G^{(2)}(t,q)$ in the self-beating mode can result in a line-width distribution $G(\Gamma)$.[20,21] For a pure diffusive relaxation, Γ is related to the translational diffusion coefficient D by $\Gamma/q^2 = D$ at $q \rightarrow 0$ and $C \rightarrow 0$, or a hydrodynamic radius R_h by $R_h = k_B T/(6\pi\eta D)$ with k_B, T, and η being the Boltzmann constant, absolute temperature, and solvent viscosity, respectively. The details of LLS instrumentation and theory can be found elsewhere.[20,21]
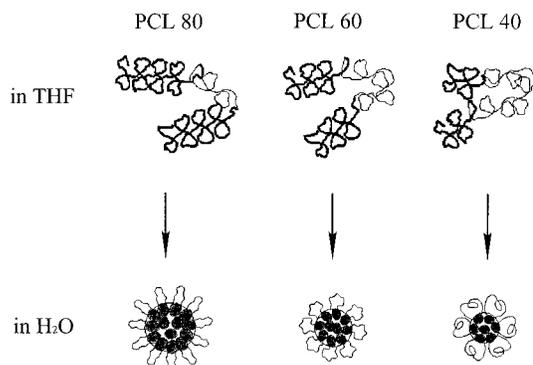
Results and Discussion

Figure 1 shows a typical plot of $KC/R_{VV}(q)$ versus q^2 for the copolymer micelles in water at $T = 20$ °C. The intercept and slope lead to $M_{w,particle}$ and $\langle R_g \rangle$, respectively. The inset shows a corresponding hydrodynamic radius distribution $f(R_h)$. The values of $M_{w,particle}$, $\langle R_g \rangle$, $\langle R_h \rangle$, and the average association number ($N_{association}$) of the copolymer chains inside each nanoparticle are summarized in Table 2. A comparison of Tables 1 and 2 shows that $\langle R_g \rangle$ is less influenced by the PEO block length but decreases as the PCL block length decreases. On the other hand, $\langle R_h \rangle$ is less affected by the length of either the PEO or PCL block. M_w clearly decreases as the PEO content increases. For the micelles made of PCL80 and PCL60, $\langle R_g \rangle/\langle R_h \rangle$ is larger than the value (0.774) predicted for a nondraining and uniform sphere, indicating that the micelles are slightly draining due to its swollen PEO shell.[18]

Figure 1. Typical plot of $KC/R_{VV}(q)$ versus q^2 for PCL60 nanoparticle in water, where K is an optical constant. The inset shows a corresponding hydrodynamic radius distribution $f(R_h)$.

TABLE 2: Light-Scattering Characterization of the PCL Micelles in Water at 20 °C, $C = 2.74 \times 10^{-6}$ g/mL[a]

sample	PCL80	PCL60	PCL40
$M_{w,particle}$	3.03×10^7	1.04×10^7	4.51×10^6
$\langle R_g \rangle$/nm	54	49	39
$\langle R_h \rangle$/nm	56	53	52
$\langle R_g \rangle/\langle R_h \rangle$	0.97	0.95	0.75
$N_{aggeregation}$	420	140	100
$\langle \rho \rangle/(g/cm^3)$	0.068	0.035	0.030

[a] Relative error: M_w, ±5%; $\langle R_g \rangle$, ±8%; $\langle R_h \rangle$, ±2%.

Figure 2. Schematic of flowerlike "core−shell" nanostructures made of triblock PCL−PEO−PCL copolymers with different chain compositions.

As a stabilizer, a longer PEO block is more effective and able to stabilize a larger surface area, so that the resultant micelles are smaller. On the other hand, for a given length of the PEO block, a longer PCL block can enhance the aggregation, leading to a larger core. Note that $\langle R_g \rangle$ is related to the chain density distribution in space. The hydrophobic PCL core is more compact than the swollen hydrophilic PEO shell, so that $\langle R_g \rangle$ decreases faster than $\langle R_h \rangle$ as the length of the PEO block increases. A simple estimation on the basis of $N_{association}$, $M_{w,PCL}$, and $M_{w,PEO}$ shows that for PCL80, PCL60, and PCL40 copolymers, the radii of the PCL cores are ~33, ~22, and ~16 nm, respectively, where an average density (~0.1 g/cm^3) of the pure PCL aggregates was used.[17] The contour lengths of the PEO blocks are ~64, ~150, and ~170 nm, respectively. A comparison of the core size, the PEO block length, and $\langle R_h \rangle$ showed that in the PCL80 micelles, the PEO blocks are stretched, while in the PCL40 micelles, the PEO blocks are in the coil state, which is schematically shown in Figure 2.

Figure 3 shows that for the PCL60 micelles, $\langle R_g \rangle$ and $M_{w,particle}$ are nearly independent of the dispersion temperature, but $\langle R_h \rangle$
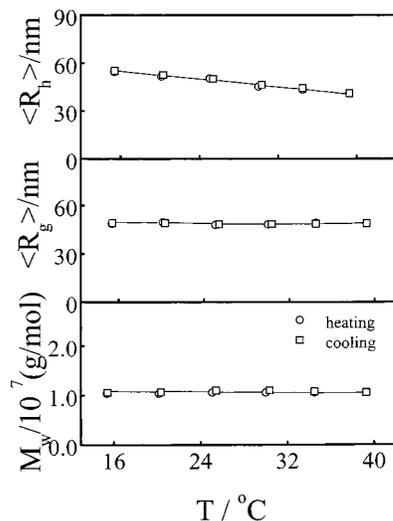
Figure 3. Typical temperature dependence of average radius of gyration ($\langle R_g \rangle$), hydrodynamic radius ($\langle R_h \rangle$) and weight-average molar mass ($M_{w,particle}$) of PCL60 micelles in water.
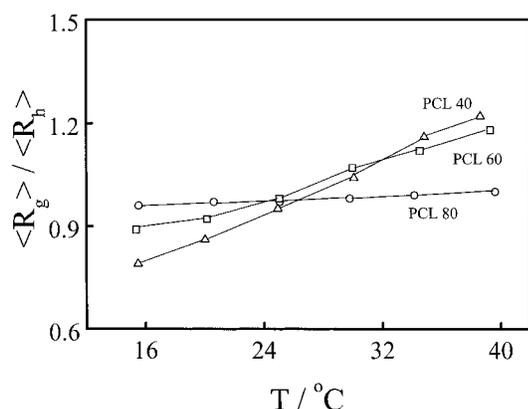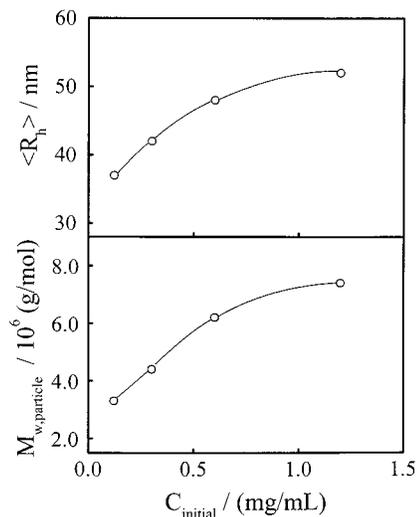

Figure 5. Initial copolymer concentration dependence of weight-average molar mass ($M_{w,particle}$) and average hydrodynamic radius ($\langle R_h \rangle$) of PCL60 micelles in water.
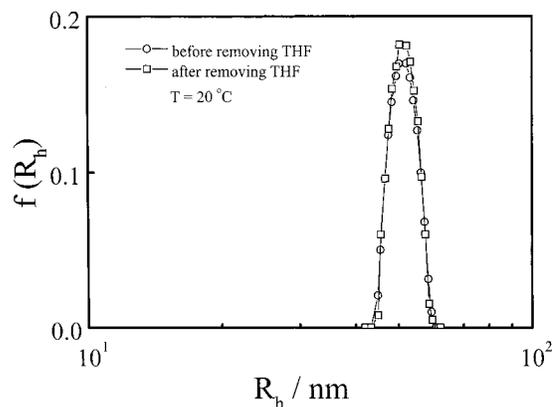

Figure 4. Temperature dependence of ratio of average radius of gyration to average hydrodynamic radius ($\langle R_g \rangle/\langle R_h \rangle$) of micelles made of different copolymer chains.

Figure 6. Comparison of hydrodynamic radius distributions $f(R_h)$ of PCL60 micelles before and after a low-pressure evaporation of 0.2% THF introduced in microphase inversion.

decreases as the temperature increases. The change of $\langle R_h \rangle$ is reversible in the cooling process. The temperature independence of $M_{w,particle}$ shows that there was no aggregation or dissolution of the micelles during heating and cooling. It is known that the solubility of PEO in water gradually decreases as the temperature increases. It is expected that the PEO block slightly shrinks as the temperature increases. Since the PCL core is much denser, a slight shrinking of the swollen PEO blocks has less effect on $\langle R_g \rangle$. Figure 4 shows a comparison of the temperature dependence of $\langle R_g \rangle/\langle R_h \rangle$ for different copolymer micelles. The increase of $\langle R_g \rangle/\langle R_h \rangle$ with the temperature is due to the decrease of $\langle R_h \rangle$. As expected, the temperature dependence becomes stronger when the PEO block is longer.

In reality, one triblock copolymer chain can undergo either an intrachain association to form a loop or an interchain bridge between two different clusters. The interchain association can be suppressed by diluting the initial THF solution and increasing the speed of the microphase inversion. To prove this point, we varied the initial copolymer concentration in THF but kept the final copolymer concentration in water as a constant. As expected, the average size and molar mass of the micelles decreases as the initial copolymer concentration in THF decreases (Figure 5). The average chain densities ($\langle \rho \rangle$) listed in Table 2 are rather lower than that of the bulk copolymer (~ 1 g/cm^3), leading to a question whether the micelles were preferentially swollen by the trace amount of THF introduced

in the microphase inversion. Figure 6 shows that removing a trace amount of THF (0.2%) introduced in the particle formation has nearly no effect on the size distribution of the micelles, ruling out the preferential adsorption. Therefore, the low values of $\langle \rho \rangle$ indicate that the nanoparticle still contains a lot of solvent in its hydrodynamic volume. To provide further evidence for this nonpreferential adsorption argument, we gradually added acetone (a good solvent for both PCL and PEO) into the dispersion.

Figure 7 shows that when the acetone content is less than $\sim 2\%$, the particles are stable in terms of $\langle R_g \rangle$, $\langle R_h \rangle$, and $M_{w,particle}$. The addition of acetone leads to the increases of $\langle R_g \rangle$ and $\langle R_h \rangle$, but not $M_{w,particle}$ in the range 0–30%. A further increase of acetone results in a sharp increase in $\langle R_g \rangle$, $\langle R_h \rangle$, and $M_{w,particle}$ before they drop at $X_{acetone} \sim 75\%$. This complicated acetone content dependence could be explained as follows. When $X_{acetone}$ content is lower than 2%, acetone uniformly mixes with water and there was no preferential adsorption inside the nanoparticle. When $X_{acetone}$ is higher, acetone gradually concentrates inside the nanoparticle and swells the PCL core. The swollen nanoparticle can be viewed as an emulsion acetone droplet. This is why $\langle R_g \rangle$, $\langle R_h \rangle$, and M_w sharply increase as $X_{acetone}$ increases. The increase of $\langle R_g \rangle$ is slower than that of $\langle R_h \rangle$, indicating that the shell swells much faster than the core. Further addition of acetone finally leads to the dissolution of the nanoparticle.
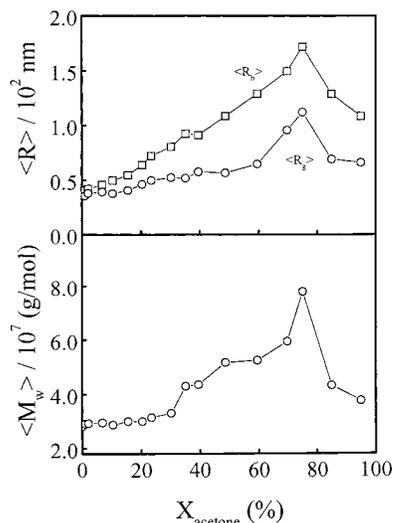
Self-Assembly of PCL−PEO−PCL

J. Phys. Chem. B, Vol. 105, No. 4, 2001 **851**

Figure 7. Acetone content dependence of average radius of gyration ($\langle R_g \rangle$), average hydrodynamic radius ($\langle R_h \rangle$), and weight-average molar mass ($M_{w,particle}$) of PCL60 micelles at 20 °C.
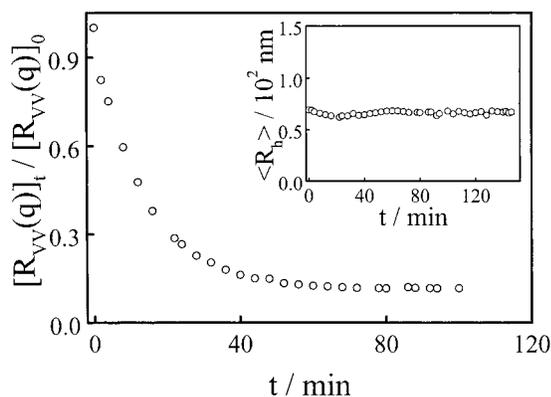

Figure 8. Biodegradation time dependence of relative Rayleigh ratio $[R_{vv}(q)]_t/[R_{vv}(q)]_0$ and average hydrodynamic radius $\langle R_h \rangle$ of PCL60 micelles at 37 °C, where the subscripts "0" and "t" represent time 0 and t, respectively; and $C_{initial} = 4.95 \times 10^{-5}$ g/mL, $C_{lipasePS} = 8.47 \times 10^{-6}$ g/mL.

Figure 8 shows the biodegradation of the PCL60 micelles in water in terms of the decrease of $[R_{vv}(q)]_t/[R_{vv}(q)]_0$ after the introduction of enzyme lipase PS. On the basis of the LLS theory, the decrease of $R_{vv}(q)$ could be attributed to either the decrease of the weight-average molar mass ($M_{w,particle}$) or the particle concentration (C). Note that laser light scattering can only "see" the remaining PCL micelles, not those small biodegradation products, mainly 5- and 6-carbon acids. The inset shows that the average hydrodynamic radius $\langle R_h \rangle$ of the remaining particles is a constant during the degradation, indicating that there was no change in $M_{w,particle}$. Therefore, the decrease of $R_{vv}(q)$ can only be attributed to the decrease of C, so that $[R_{vv}(q)]_t/[R_{vv}(q)]_0 = C_t/C_0$. A combination of static and

dynamic LLS results in Figure 8 indicates that the biodegradation of each nanoparticle is fast and lipase PS degrades the micelles in a one-by-one fashion. The degradation rate can be well controlled in the range of a few minute to a few days or even longer. The details of the biodegradation results will be reported later.

Conclusions

The self-assembly of triblock copolymer poly(caprolactone-*b*-oxide ethylene-*b*-caprolactone) (PCL−PEO−PCL) chains can be induced by adding its THF solution dropwise into an excess of water via a microphase inversion. After a proper suppressing of the interchain bridging, most of the insoluble PCL blocks can undergo an intrachain association prior to the interchain assembly into a flowerlike nanostructure with a collapsed biodegradable PCL core and a swollen shell made of small PEO loops. The particle size and the association number can be well controlled by the initial copolymer composition and concentration in THF. The PEO shell shrinks as the temperature increases and the micelles are stable at body temperature, which is an important parameter for their biomedical applications.

References and Notes

(1) Hadziioannou, G.; Patel, S.; Granick, S.; Tirrell, M. *J. Am. Chem. Soc.* **1986**, *108*, 2869.

(2) Milner, S. T. *Science* **1991**, *251*, 905.

(3) Zhu, P. W.; Napper, D. H. *J. Colloid Interface Sci.* **1994**, *164*, 489.

(4) Yu, K.; Eisenberg, A. *Macromolecules* **1998**, *31*, 3509.

(5) Zhang, L.; Eisenberg, A. *Science* **1995**, *268*, 1728.

(6) Balsara, N. P.; Tirrell, N.; Lodge, T. P. *Macromolecules* **1991**, *24*, 1975.

(7) Wu, G.; Chu, B. *Macromolecules* **1994**, *27*, 1766.

(8) Mortensen, K.; Brown, W. *Macromolecules* **1993**, *26*, 4128.

(9) Wu, C.; Gao, J. *Macromolecules* **2000**, *33*, 645.

(10) Zhou, Z.; Chu, B. *Macromolecules* **1994**, *27*, 2025.

(11) Zhou, Z.; Chu, B.; Nace, V. M.; Yang, Y. W.; Booth, C. *Macromolecules* **1996**, *29*, 3663.

(12) Zhou, Z.; Chu, B.; Nace, V. M. *Langmuir* **1996**, *12*, 5016.

(13) Liu, T.; Zhou, Z.; Wu, C.; Chu, B.; Schneider, D. K.; Nace, V. M. *J. Phys. Chem. B* **1997**, *101*, 8808.

(14) Schmolka, I. R. In *Polymers for Controlled Drug Delivery*; Tarcha, P. J., Ed.; CRC Press: Boston, 1992.

(15) Schmolka, I. R. *Am. Perfume Cosmet.* **1967**, *82*, 25.

(16) Chen-chow, P.-C.; Frank, S. G. *Int. J. Pharm.* **1981**, *8*, 89.

(17) Gan, Z.; Jim, T. F.; Li, M.; Zhao, Y.; Wang, S.; Wu, C. *Macromolecules* **1999**, *32*, 590.

(18) Zhao, Y.; Hu, T.; Lv, Z.; Wang, S.; Wu, C. *J. Polym. Sci. Polym. Phys. Ed.* **1999**, *37*, 3288.

(19) Wang, S.; Qin, B. *Polym. Adv. Technol.* **1993**, *4*, 363.

(20) Chu, B. *Laser Light Scattering*, 2nd ed.; Academic Press: New York, 1991.

(21) Berne, B.; Pecora, R. *Dynamic Light Scattering*, 2nd ed.; Plenum Press: New York, 1991.